JMEPEG (2012) 21:2451–2459
DOI: 10.1007/s11665-012-0187-2

1059-9495/$19.00

Influence of the Strength Mismatch of a Narrow Gap Welded Joint of SA508 on the Plastic η Factor

J.M. Koo, Y. Huh, and C.S. Seok

(Submitted August 10, 2011; in revised form January 26, 2012)

In this article, the influence of the strength mismatch of a narrow gap welded joint of SA508 on the η factor was evaluated. The η factor is the principal parameter that determines the plastic portion of the *J*-integral. The specimens for tensile and hardness tests were collected from piping with narrow gap welding and the stress-strain curve and hardness were obtained from those. From these results, the Ramberg-Osgood (R-O) constant was obtained. Also, the finite element analysis was performed with variations in the strength mismatch and the weld width. The η factor equation considering the strength mismatch and the weld width of a narrow gap welded joint was suggested.

Keywords fracture toughness, *J*-integral, narrow gap welded joint, Plastic component, Ramberg-Osgood constant, strength mismatch

1. Introduction

The use of narrow gap welding for the piping of large-scale structures, such as nuclear power plants, has recently increased. Since the weld width by narrow gap welding is smaller than that by general welding, this method has an advantage of decreasing the shrinkage and deformation of the weld part, and lowering the residual stresses, due to the reduction of the welding time. Most studies on such narrow gap welding have focused on evaluating the weld integrity. In particular, some of the efforts have been on leak-before-break (LBB) analysis, which is essential to the design of the piping in nuclear power plants (Ref 1, 2).

In case of general welding, effects of strength differences (mismatch) between weld metal and two base metals, as well as local variations of strength within weld HAZ zones, on the fracture toughness properties of welded joints were observed, due to high global weld joint mismatch (Ref 3). Oh et al. (Ref 4) performed the quantification for the effect of geometry and crack location on crack driving force for welded joints, via systematic elastic-creep and elastic-plastic finite element analyses (FEA) for welded joints and reported that their equivalent material concept works very well only for a planar geometry with an internal crack and for a planar geometry with an edge crack, it tends to provide conservative results for under-matching and for interface cracks. Also, for a cylindrical geometry with an edge crack, it was reported that the results are similar to those for a planar geometry with an edge crack, but caution should be exercised for over-matching, as non-conservative estimates are possible due to gross-section yielding.

J.M. Koo, Y. Huh, and **C.S. Seok**, School of Mechanical Engineering, Sungkyunkwan University, 300 Cheoncheon-dong, Suwon, Gyeonggi-do 440-746, Republic of Korea. Contact e-mail: seok@skku.edu.

In this article, the influence of the strength mismatch of a narrow gap welded joint of a compact tension (CT) specimen of SA508 on the η factor was evaluated. In order to perform it, the specimens for tensile and hardness tests were collected from piping with narrow gap welding and the stress-strain curve and hardness were obtained from those. From these results, the Ramberg-Osgood (R-O) constant was obtained. Also, the FEA was performed according to a variation of the strength mismatch and the weld width. From the results, the η factor equation considering the strength mismatch and the weld width of a narrow gap welded joint was suggested. In addition, the fracture toughness (*J-R* curve) test was performed to verify the proposed equation.

1.1 J-Integral and Strength Mismatch

In case the of the plane strain, the *J*-integral by ASTM E1820 (Ref 5) can be determined by superposing the elastic component J_{el} and the plastic component J_{pl} as follows:

$$J = J_{el} + J_{pl} \quad \text{(Eq 1)}$$

where

$$J_{pl} = \frac{\eta A_{pl}}{B_N b} \quad \text{(Eq 2)}$$

$$\eta = 2 + 0.522(b/W) \quad \text{(Eq 3)}$$

where η, called the η factor, is a dimensionless constant; A_{pl} is the plastic area of the load-displacement curve; B_N is the depth for subtracting a side groove from the total thickness; and b is the residual ligament.

Many studies have evaluated the weld integrity by using the strength mismatch ratio of the base metal and the weld part (Ref 6-8).

In general, the strength mismatch ratio of the base metal and the weld part, called the mismatch factor, M_W is as follows (Ref 6-8):

$$M_W = \frac{\sigma_{YW}}{\sigma_{YB}} \quad \text{(Eq 4)}$$

where σ_{YB} and σ_{YW} are the yield strengths of the base metal and the weld part, respectively. $M_W = 1$ occurs when the weld has the same yield strength as the base metal, which is called even-match. $M_W > 1$ occurs when the yield strength of the base metal is lower than that of the weld part, which is commonly called an over-match. $M_W < 1$ occurs when the yield strength of the base metal is higher than that of the weld part, which is called an under-match. However, these do not consider the effect of the heat-affected zone (HAZ) on the weld part. In this study, the effect of the HAZ was considered in terms of the strength mismatch ratio of the base metal and the HAZ, as shown in Eq 5.

$$M_H = \frac{\sigma_{YH}}{\sigma_{YB}} \quad \text{(Eq 5)}$$

where σ_{YH} is the yield strength of the HAZ.

2. Tensile and Hardness Test

2.1 Materials and Specimens

The materials used in this study were SA508 Cl.1a and SA508 Cl.3a carbon steel. These materials are often used for first stage piping in nuclear power plants. The pipes were 1000 mm in diameter with a wall thickness of 100 mm, and were manufactured by narrow gap welding. Table 1 shows the chemical composition of the materials, and Table 2 shows the welding conditions.

Table 1 Chemical composition of materials

	C	Si	Mn	P	S	Ni	Cr	Mo
SA508 Cl.1a	0.2	0.22	1.15	0.01	0.002	0.22	0.096	0.056
SA508 Cl.3a	0.19	0.08	1.35	0.006	0.002	0.83	0.17	0.009

Table 2 Weld conditions

	Filler metal	
Weld method	**AWS class**	**Size, mm**
GTAW (machine weld)	ER70S-6	∅0.9

The mechanical properties were obtained from tensile test specimens collected from a real pipe according to ASTM E8 (Ref 9), but those of the HAZ were obtained from the micro-Vickers hardness test with the specimen, as shown in Fig. 1.

2.2 Strength Characteristics

The tensile test was performed at room temperature according to ASTM E8, and the test speed was 1 mm/min. Table 3 shows the results of the tensile test.

The base metal, the weld part, and the HAZ of the hardness specimen were identified by etching. The surfaces were polished so that indentation impressions could be clearly observed. A micro-Vickers hardness test was performed according to ASTM E384 (Ref 10). The test load was 19.62 N and the holding time was 12 s during loading. The indentations were conducted five times per part. Figure 2 and Table 4 show the results of the hardness test.

The hardness value of the HAZ was about 5-10% higher than that of the base metal and the hardness values of a quarter and the center of a weld part were almost the same.

3. Determination of the R-O Constant by Yield Strength

To evaluate the plastic η factor, the strength mismatch of a narrow gap welded joint was considered. To obtain the R-O constant based on the variation of the yield strength, tensile tests were performed.

Figure 3 shows the true stress-true strain curves for SA508 Cl.1a, SA508 Cl.3a, and the weld part. The R-O equation

Table 3 Results of the tensile test

			Ramberg-Osgood constant	
Material	**Yield strength, MPa**	**Ultimate strength, MPa**	**α**	***n***
Weld	397.7	645.0	3.386	5.188
SA508 Cl.1a	330.4	517.9	5.280	4.845
SA508 Cl.3a	499.3	645.6	2.622	7.727

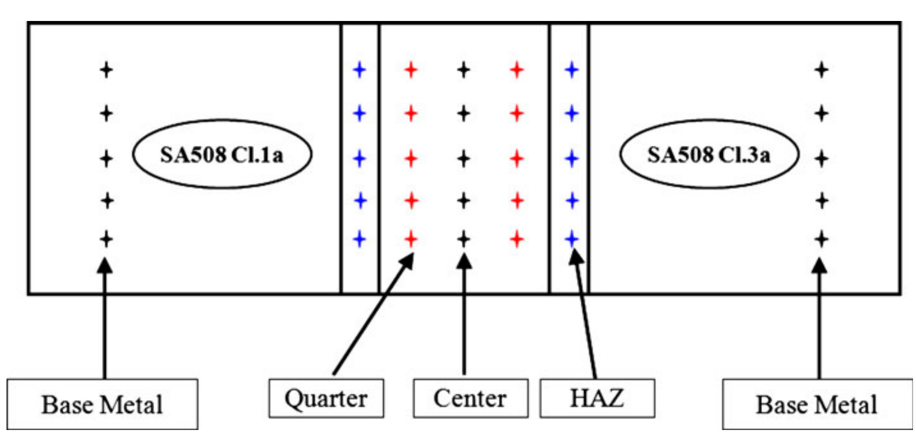

Fig. 1 The schematic of the micro-Vickers hardness test specimen

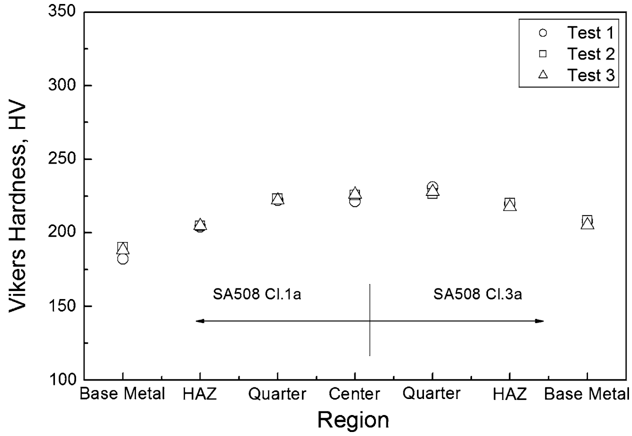

Fig. 2 Distribution of the Vickers hardness values

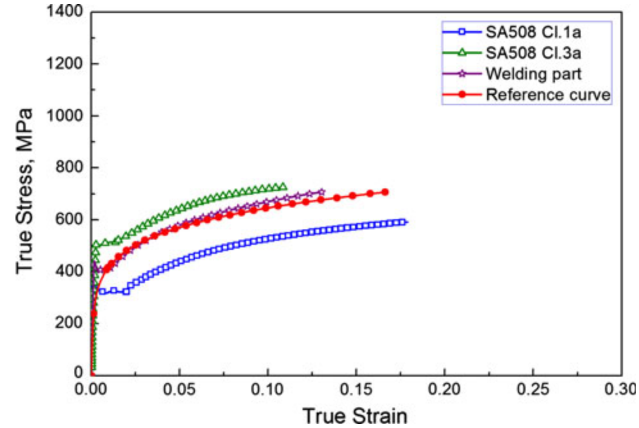

Fig. 3 True stress-true strain curve of base metals and weld part and reference curve

Table 4 Summary of the hardness test results

		Vickers hardness (HV)		
Direction	**Region**	**1st**	**2nd**	**3rd**
SA508 Cl.1a	Base metal	192.2	199.9	198.3
	HAZ	204.2	204.6	204.7
Welding	Quarter	222.0	223.1	222.1
	Center	221.3	225.6	226.1
	Quarter	230.9	226.6	227.9
SA508 Cl.3a	HAZ	202.0	202.1	203.4
	Base metal	197.7	200.5	197.1

for the stress-strain relationship of elastic-plastic materials is (Ref 11)

$$\frac{\varepsilon}{\varepsilon_0} = \frac{\sigma}{\sigma_0} + \alpha\left(\frac{\sigma}{\sigma_0}\right)^n \quad \text{(Eq 6)}$$

where σ_o, ε_0, and, n are the yield strength, strain, and the strain hardening exponent, respectively. The values of α and n for each part were obtained from the tensile data. As the yield strength is fixed at 400 MPa and the R-O constants α and n were changed, a reference curve that was similar to the true stress-true strain curve of the weld part was sought, as shown in Fig. 3. Figure 4 shows the offset results of the reference curve according to variation of yield strength. Using Eq 6, α and n for the offset reference curve were obtained. Equation 7 was obtained by fitting n to the yield strength. After a value of n was obtained from Eq 7 again, a value of α was extracted from Eq 6 and Eq 8 was obtained by fitting α.

$$n = 0.01\sigma_0 + 1.8 \quad \text{(Eq 7)}$$

$$\alpha = 196.7\sigma_o^{-0.7} \quad \text{(Eq 8)}$$

4. FEA for Evaluation of the Plastic η factor

4.1 FEA Model

To evaluate the plastic η factor using the strength mismatch, 3-D FEA models with a thickness of 1T were constructed under

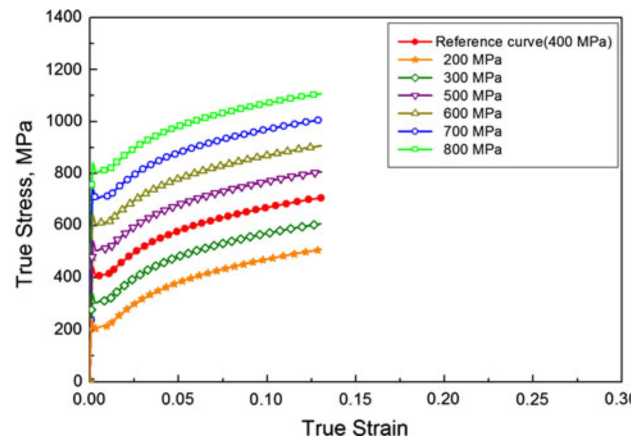

Fig. 4 Reference curve offset

variations of the weld part and the HAZ width (see Fig. 5). The analysis was performed using ABAQUS Ver.6.7. In this study, the weld part and the HAZ width of narrow gap welding were about 16 and 4 mm respectively. Therefore, in order to verify the effect of the weld part and the HAZ width, the HAZ width was fixed at 4 mm while the weld width was varied from 8 to 32 mm and the weld width was fixed at 16 mm while the HAZ width was changed from 2 to 8 mm (Table 5).

The FEA model was very densely structured at the crack tip and was composed of about 4000 elements and 21,000 nodes by the use of a 20-node quadratic brick integration element (C3D20). It was assumed that the mechanical properties for the FEA would satisfy the requirements of the R-O equation and Table 6 shows the mechanical properties. The *J*-integral was calculated from the FEA results using an area integral method provided by ABAQUS.

In order to verify the model, the results from the FEA for the homogeneous materials were compared with the plastic η factors from Eq 3 in ASTM E1820, as shown in Fig. 6.

The results agree well with each other with a maximum deviation of 3%.

In this study, in order to evaluate the influence of the width and the strength of the weld part and the HAZ on the plastic η factor, the FEA was performed with variation of the weld width and the strength mismatch ratios (see Table 7, 8). Also, the R-O

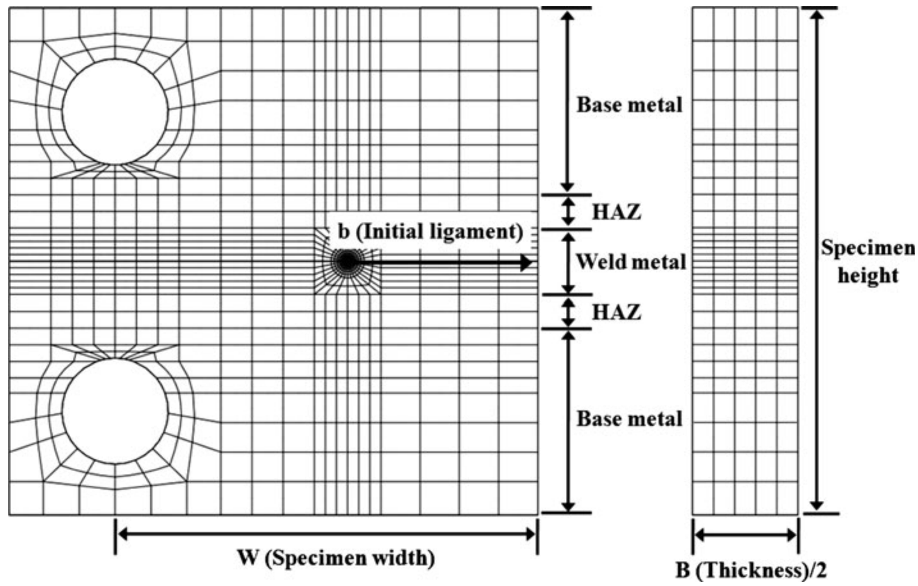

Fig. 5 FEA model for the strength mismatch

Table 5 Dimensions of the model for analysis

b/W	B	W	b	HAZ width, mm				Weld width, mm			
0.50	25.4	50.8	25.40	4				8	16	24	32
0.55	25.4	50.8	22.86	4				8	16	24	32
0.60	25.4	50.8	20.32	4				8	16	24	32
0.65	25.4	50.8	17.78	4				8	16	24	32
0.70	25.4	50.8	15.24	4				8	16	24	32
0.50	25.4	50.8	25.40	2	4	6	8	16			
0.55	25.4	50.8	22.86	2	4	6	8	16			
0.60	25.4	50.8	20.32	2	4	6	8	16			
0.65	25.4	50.8	17.78	2	4	6	8	16			
0.70	25.4	50.8	15.24	2	4	6	8	16			

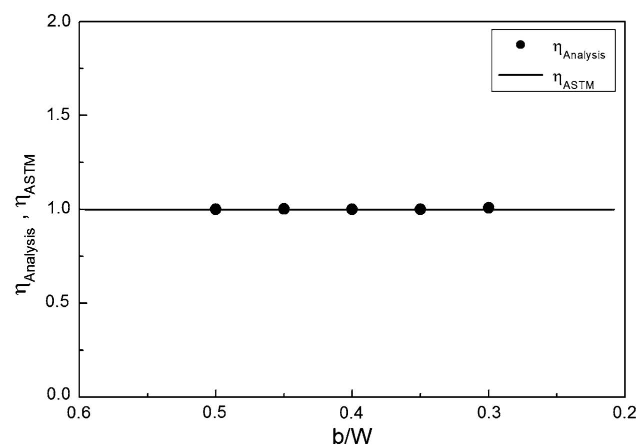

Fig. 6 Verification of the FEA model

Table 6 Mechanical properties for FEA

Region	Young's modulus, GPa	Poisson's ratio	Yield strength, MPa	Ramberg-Osgood constant	
				α	n
SA508 C1.1a	200	0.3	330.4	4.845	5.280
SA508 C1.3a			499.3	7.727	2.622
Weld			397.7	5.188	3.386
HAZ			361.6	5.018	5.386

constants that were calculated by Eq 7 and 8 were applied to the FEA.

4.2 Evaluation of the Plastic η Factor with the Strength Mismatch of HAZ

In order to evaluate the influence of the strength mismatch of the HAZ on the plastic η factor, FEA was performed with variation of M_H. Figures 7 to 10 show the comparison between the FEA results and those from Eq 3.

Figure 7 shows the analysis results for M_H from 0.8 to 1.2. Since the deviation of the analysis results according to variation of strength mismatch ratio is below 3%, the effect of the strength mismatch of the HAZ on the factor slightly appears. Figures 8 and 9 show the relationships between the plastic η factor and b/W according to variation of the weld width when M_H is 1.1, and the yield strengths of the parts excepting the HAZ are 330 and 500 MPa. When the weld width increases, the analysis results tend to decrease and the maximum deviation is about 2%. Figure 10 shows the relationships between the plastic η factor and the b/W according to variation of the HAZ width when M_H is 1.1 and the yield strengths of the parts excepting the HAZ are 330 MPa. When the width of the HAZ increases, the analysis results tend to decrease and the maximum deviation is about 3%. Therefore, it can be seen that the effects of the HAZ on the plastic η factor are small regardless of M_H and the weld and HAZ widths (at M_H = 1.1). The minimal effect of the HAZ is possibly because the width of the HAZ is smaller than that of the base metal or the weld part. Therefore, when evaluating the strength mismatch of a narrow

Table 7 Summary of the results from FEA for various values of the strength mismatch ratio between the base metal and the HAZ (M_H)

M_H	σ_{YB}, MPa	σ_{YW}, MPa	σ_{YH}, MPa	HAZ width, mm	Weld width, mm
0.8	330	330	264	4	16
0.9	330	330	297	4	16
1.2	330	330	396	4	16
1.1	330	330	363	4	8 16 24 32
1.1	500	500	550	4	8 16 24 32
1.1	330	330	363	2 4 6 8	16

Table 8 Summary of the results from FEA for various values of the strength mismatch ratio between the base metal and the weld part (M_W)

M_W	σ_{YB}, MPa	σ_{YW}, MPa	σ_{YH}, MPa	HAZ width, mm	Weld width, mm
0.60	330	363	200	4	8 16 24 32
0.75	330	363	248	4	8 16 24 32
0.90	330	363	300	4	8 16 24 32
1.20	330	363	400	4	8 16 24 32
1.50	330	363	500	4	8 16 24 32
1.80	330	363	600	4	8 16 24 32

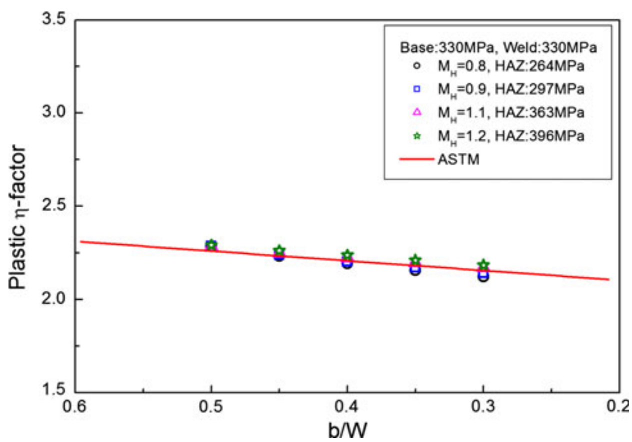

Fig. 7 Relationship between the plastic η factor and b/W for various M_H values

gap welded joint, it is thought that the effect of the HAZ may be disregarded.

4.3 Evaluation of the Plastic η Factor with the Strength Mismatch of Weld Part

Figure 11 shows the analysis results for variation of the M_W at 16 mm in weld width. When $M_W > 1$, the results tend to be smaller than those from Eq 3 in ASTM E1820 but when $M_W < 1$, those shows a reverse tendency.

As M_W approaches 1, i.e., as the strength of the weld part becomes similar to that of the base metal, the plastic η factor of the weld joint approaches that of the homogeneous materials.

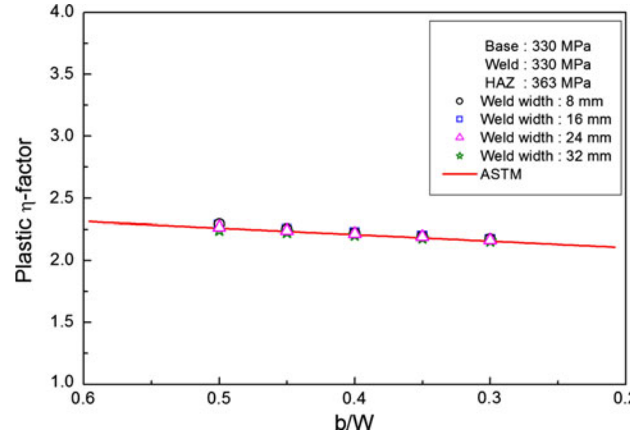

Fig. 8 Relationship between the plastic η and b/W for various weld width values (M_H = 1.1)

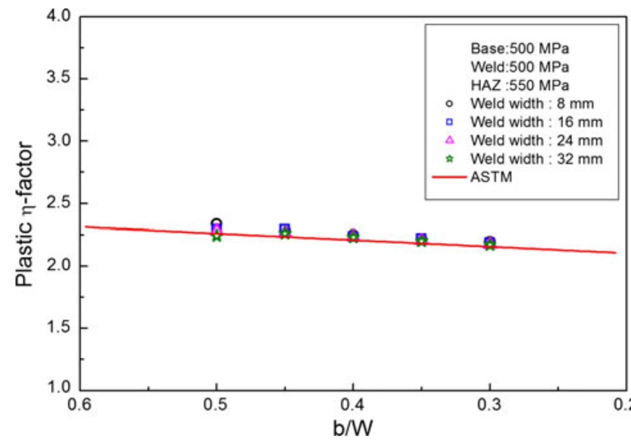

Fig. 9 Relationship between the plastic η factor and b/W for various weld width values (M_H = 1.1)

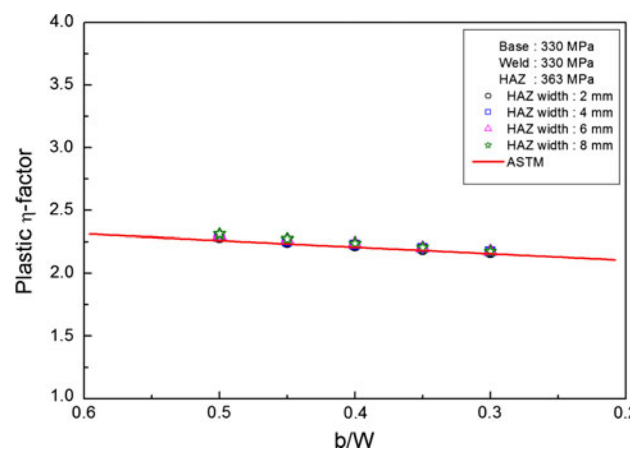

Fig. 10 Relationship between the plastic η factor and b/W for various HAZ width values (M_H = 1.1)

When M_W varies from 0.6 to 1.8 at $b/W = 0.5$, the maximum deviation of the analysis results is about 40%, and in the case of $M_W = 0.6$, since the deviation between the analysis results and Eq 3 is about 17%, M_W should be considered. In the case of over- and under-match, the analysis results tend to decrease as

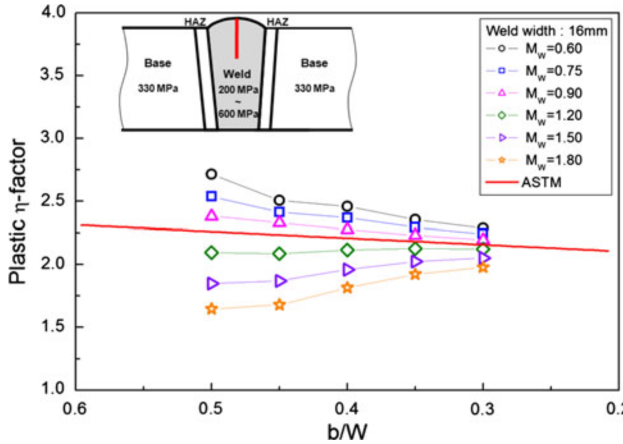

Fig. 11 Relationship between the plastic η factor and b/W for various strength mismatch (weld width = 16 mm)

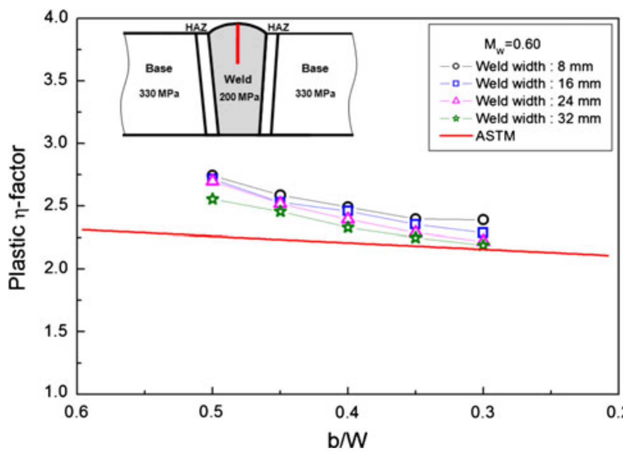

Fig. 12 Relationship between the plastic η factor and b/W for weld width ($M_W = 0.6$)

M_W increases and approach those of Eq 3 when the crack length increases.

4.4 Evaluation of the Plastic η Factor for Variation of Weld Width

Figure 12 shows the analysis results for variation of weld width at $M_W = 0.6$. The analysis results for a weld width of 8 mm are about 8% larger than those for a weld width of 32 mm at $b/W = 0.5$ and about 17% larger than the results that are based on Eq 3. Thus, it is confirmed that the plastic η factor is affected by the weld width and that the weld width should be considered in the case of narrow gap welding.

Figures 13, 14, and 15 show the analysis results for the variation of M_W in the case of 8, 24, and 32 mm, respectively, in weld width. At a weld width 8 mm, the plastic η factors decrease according to a decrease of b/W, but even if b/W is <0.3, those do not converge on Eq 3. In the case of weld widths of 24 and 32 mm, the analysis results decrease according to a decrease of b/W, and at $b/W = 0.3$ (15.24 mm), the plastic η factors converge on Eq 3.

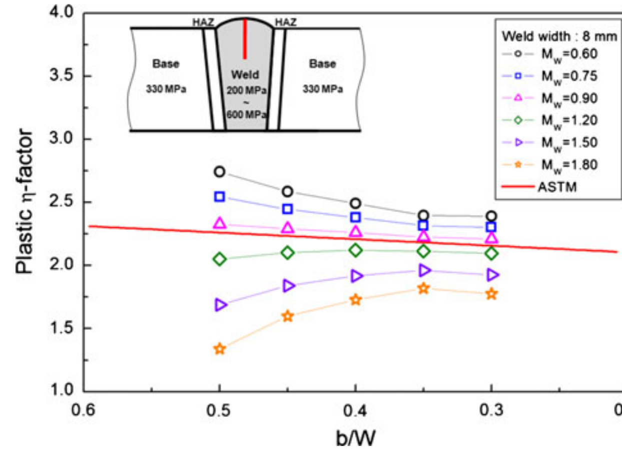

Fig. 13 Relationship between the plastic η factor and b/W for strength mismatch (weld width = 8 mm)

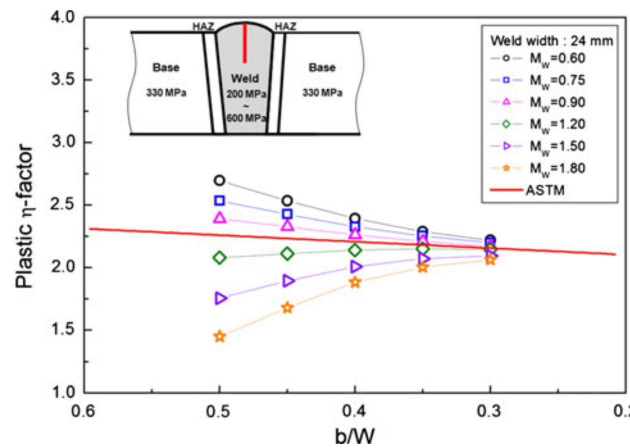

Fig. 14 Relationship between the plastic η factor and b/W for strength mismatch (weld width = 24 mm)

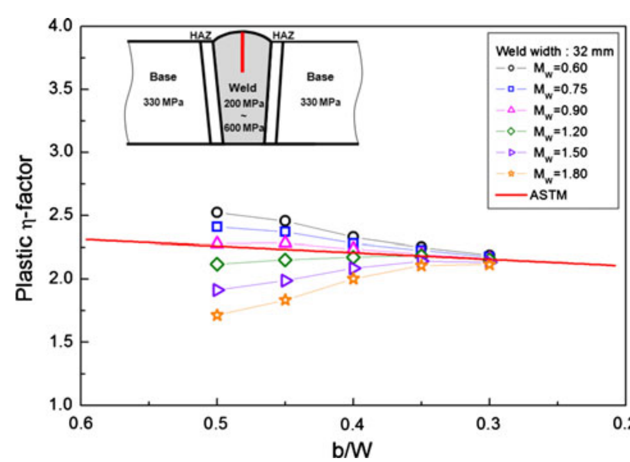

Fig. 15 Relationship between the plastic η factor and b/W for strength mismatch (weld width = 32 mm)

5. A New Plastic η Factor Equation that Considers Variations in the Strength Mismatch and the Weld Width

From the fact that an intersection of the lines of fitting the analysis results according to variation of M_W are located on the line of Eq 3 as shown in Fig. 16, the new plastic η factor equation is suggested. That is, an intersection located at $b/W = 0.21$ and $\eta = 2.11$ is used, and the equations for the plastic η factor are suggested as follows:

$$\eta = S[(b/W) - 0.21] + 2.11 \quad \text{(Eq 9)}$$

$$S = g(M_W - 1) + 0.522 \quad \text{(Eq 10)}$$

where S is the slope for the variation of M_W. In Eq 9, if $b/W = 0.21$, η becomes 2.11, and in the case of $M_W = 1$, S in Eq 10 becomes the slope of Eq 3 in ASTM E1820, 0.522. Figure 17 shows the relationships between M_W and S for various weld widths. By fitting these points, the slopes, namely, g_8, g_{16}, g_{24}, and g_{32} for the weld widths, 8, 16, 24, and 32 mm, respectively, are obtained.

The specimen height by ASTM E1820 is 1.2 W and if ω from Eq 11 reaches 1.2 as the weld width widens, all materials become base metals. In this study, the slopes, namely, g_8, g_{16}, g_{24}, and g_{32}, for various weld widths, are plotted against ω. The relationship between g and ω, whereby g vanishes when ω is 1.2, is obtained as follows:

$$\omega = \frac{W_{\text{weld width}}}{W_{\text{specimen height}}} \quad \text{(Eq 11)}$$

$$g = 3.43(\omega - 1.2) \quad \text{(Eq 12)}$$

Finally, the equation for the plastic η factor that considers the strength mismatch ratio and the weld width is proposed as follows:

$$\eta = [3.43(\omega - 1.2)][(M_W - 1) + 0.522][(b/W) - 0.21)] + 2.11 \quad \text{(Eq 13)}$$

To verify the suggested plastic η factor equation, FEA was performed and the plastic η factor from the FEA was compared with that from the suggested equation. The results are shown in Fig. 18 to 21. When the weld is 32 mm in weld width, the results from the FEA and Eq 13 agree within 5%, while at 8 mm they are nearly similar. Therefore, it can be seen that the suggested plastic η factor equation for narrow gap welding is valid. Also, it is thought that the fracture toughness of similar welding materials can be easily and accurately determined when only the yield strength is known.

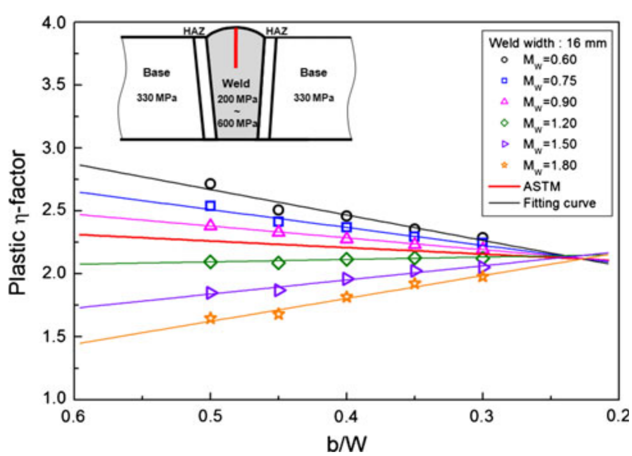

Fig. 16 Curve fitting for the plastic η factor

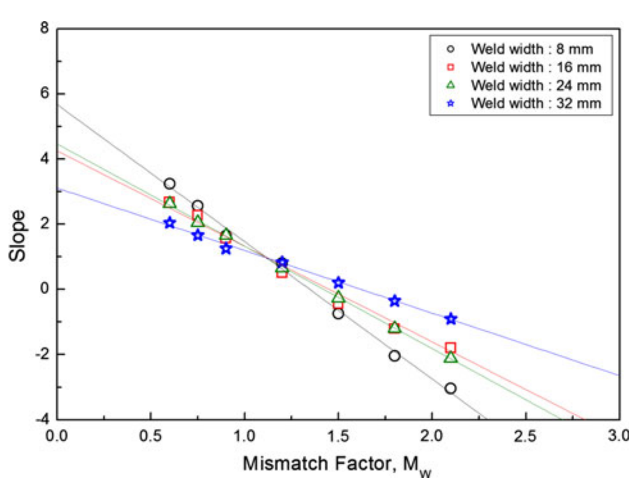

Fig. 17 Curve fitting for the slope

6. Evaluation of Fracture Toughness by Applying the New Plastic η Factor Equation

6.1 Fracture Toughness Test

Fracture toughness tests by the single specimen method according to ASTM E1820 were performed to the evaluation of the fracture toughness by applying the new plastic η factor equation. 1T-CT standard specimens with the thickness of 25.4 mm and the weld width of 16 mm were collected from the SA508 Cl.1a pipe with the narrow gap welding part.

Fracture toughness tests were performed at 316 °C, i.e., the design temperature for the primary piping system of nuclear power plants, and test speed was 1 mm/min. The notch tip was sharpened by fatigue pre-cracking. Also the crack length was measured by the unloading compliance method.

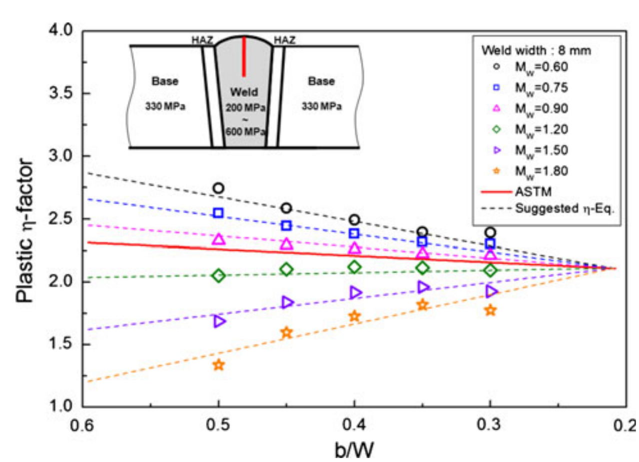

Fig. 18 Verification of the suggested plastic η factor equation (weld width = 8 mm)

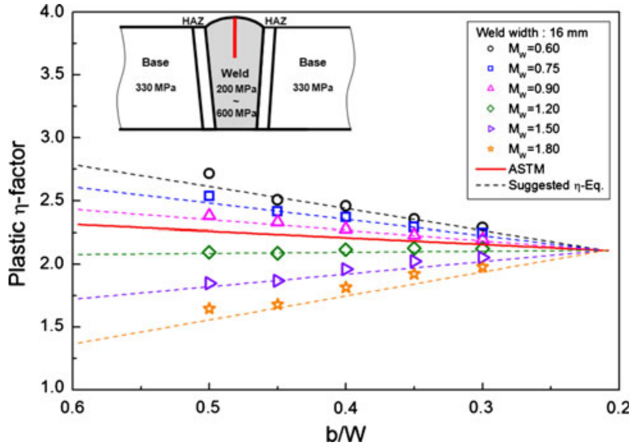

Fig. 19 Verification of the suggested plastic η factor equation (weld width = 16 mm)

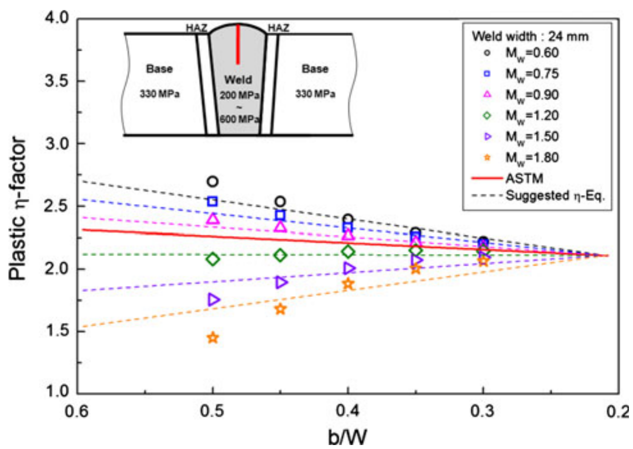

Fig. 20 Verification of the suggested plastic η factor equation (weld width = 24 mm)

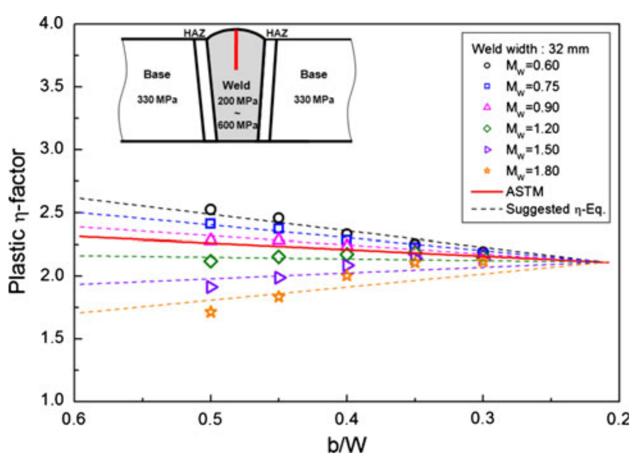

Fig. 21 Verification of the suggested plastic η factor equation (weld width = 32 mm)

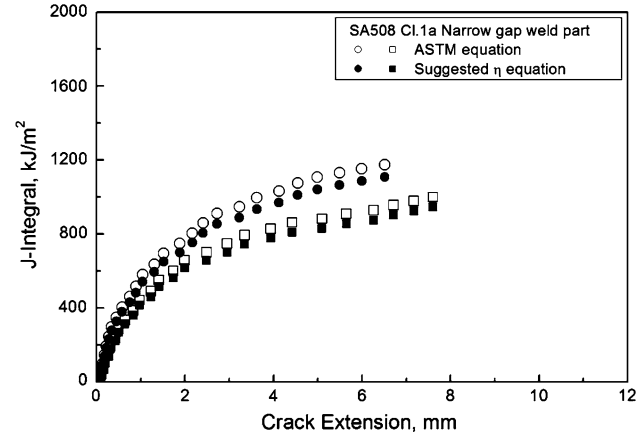

Fig. 22 Comparison of *J-R* curves between ASTM and suggested plastic η factor equation

Table 9 Summary of fracture toughness test results

Plastic η factor	Test temp., °C	Specimen no.	Weld width, mm	J_{IC}, kJ/m^2
ASTM (Eq 3)	316	508NGW-J1	16	482.5
		508NGW-J2		302.5
New (Eq 14)	316	508NGW-J1	16	422.3
		508NGW-J2		313.3

6.2 Application of the New Plastic η Factor Equation

The yield strengths of the base metal and the weld part used in this study are about 330 and 398 MPa, respectively. So, the strength mismatch is about 1.21, and the weld width is about 16 mm. When two parameters are applied to the new plastic η factor of Eq 13, the plastic η factor becomes as follows:

$$\eta = 2.140 - 0.141(b/W) \qquad \text{(Eq 14)}$$

Figure 22 shows to make a comparison between *J-R* curve by Eq 14 and by 3. The *J*-integral by Eq 14 is less than that by ASTM E1820 and the maximum deviation of them is about 6%. Table 9 shows the results of facture toughness tests and it is noted that the fracture toughness obtained from Eq 14 is lower than that obtained from Eq 3.

The specimen with the narrow gap welding par used in this study is the case of over-matching that the strength mismatch is >1. Therefore, it can be estimated that the fracture toughness by Eq 14 is lower than that by ASTM E1820.

7. Conclusion

The influence of the strength mismatch of a narrow gap welded joint on the plastic η factor was evaluated. The FEA was performed to evaluate the strength mismatch and the plastic η factor for various weld widths was evaluated. Based on these analyses, the plastic η factor considering the strength mismatch of a narrow gap welded joint was proposed. Also the fracture toughness tests for the SA508 Cl.1a specimen with the narrow gap welding part were performed and then the fracture toughness by the new plastic η factor equation was compared with that by ASTM E1820.

The conclusions are as follows:

(1) Since the effects of the HAZ regardless of M_H and the weld and the HAZ width (at $M_H = 1.1$) on the plastic η factor are small, when evaluating the strength mismatch of a narrow gap welded joint, it is thought that the effect of the HAZ may be disregarded.
(2) The plastic η factor is affected by the strength mismatch and the weld width; hence, the strength mismatch and the weld width should be considered in the case of narrow gap welding.
(3) A plastic η factor regarding the strength mismatch and the weld width for narrow gap welding is suggested. The plastic η factor that is derived from FEA is compared with that which is based on the suggested equation. From these results, it can be seen that the suggested plastic η factor equation for narrow gap welding is valid.
(4) The fracture toughness obtained with the new plastic η factor equation is lower than that obtained from ASTM E 1820 because the new plastic η factor equation evaluates the fracture toughness by considering the strength mismatch. Therefore, the new plastic η factor equation can improve the conservative estimates of the fracture toughness by ASTM E1820.

Acknowledgments

This work has been supported by the Brain Korea 21 Project and the Korea Science and Engineering Foundation (KOSEF). Grant funded by the Korea government (MOST) (No. 2007-03205)

References

1. J.-S.Yang, C.-Y. Park, and N.-S. Huh, Estimates of Mechanical Properties and Residual Stress of Narrow Gap Weld for Leak-Before-Break Application to Nuclear Piping, J. Press. Vessel Technol. Trans. ASME, 2011, **133**(2), art. no. 021403
2. C. Jang, P.Y. Cho, M. Kim, S.J. Oh, and J.S. Yang, Effects of Microstructure and Residual Stress on Fatigue Crack Growth of Stainless Steel Narrow Gap Welds, *Mater. Des.*, 2010, **31**, p 1862–1870
3. I. Rak and A. Treiber, Fracture Behaviour of Welded Joints Fabricated in HSLA Steels of Different Strength Level, *Eng. Fract. Mech.*, 1999, **64**, p 401–415
4. C.-K. Oh, Y.-J. Kim, J.-M. Park, J.-S. Kim, and T.-E. Jin, Effect of Structural Geometry and Crack Location on Crack Driving Forces for Cracks in Welds, *Eng. Fract. Mech.*, 2007, **74**, p 912–931
5. Standard Test Method for Measurement of Fracture Toughness,'' ASTM E 1820-11, ASTM
6. S. Hao, K.H. Schwalbe, and A. Cornec, The Effect of Yield Strength Mis-Match on the Fracture Analysis of Welded Joints: Slip-Line Field Solutions for Pure Bending, *Int. J. Solids Struct.*, 2000, **37**, p 5385–5411
7. T.-K. Song, Y.-J. Kim, J.-S. Kim, and T.-E. Jin, Mismatch Limit Loads and Approximate J Estimates for Tensile Plates With Constant-Depth Surface Cracks in the Center of Welds, *Int. J. Fract.*, 2007, **148**, p 343–360
8. S. Rahman, F. Brust, N. Ghadiali, and G. Wilkowski, Crack-Opening-Area Analyses for Circumferential Through-Wall Cracks in Pipes—Part I: Analytical Models, *Int. J. Press. Vessels Pip.*, 1998, **75**, p 357–373
9. ''Standard Test Methods for Tension Testing of Metallic Materials,'' ASTM E 8-01, ASTM
10. ''Standard Test Method for Micro- indentation Hardness of Materials,'' ASTM E 384-99, ASTM
11. W. Ramberg and W.R. Osgood, Description of Stress-Strain Curves by Three parameters, NACA-TN-902, NACA, 1943